

Zn Concentration, Shape and Size Effects on the Band Structure of Photonic Crystals Based on Ferrofluids with $(\text{Co}_{1-x}\text{Zn}_x\text{Fe}_2\text{O}_4)$ Nanoparticles

Luz E. González and N. Porrás-Montenegro

Departamento de Física, Universidad del Valle, A.A. 25360, Cali, Colombia

Abstract— In this work using the transfer matrix technique we study the Zn concentration, nanoparticles size and shape effects on the band structure of a 1D photonic crystal (PC), made of alternating layers of air and a ferrofluid containing $(\text{Co}_{1-x}\text{Zn}_x\text{Fe}_2\text{O}_4)$ nanoparticles, coated by oleic acid suspended in ethanol. We found that the photonic band structure (PBS) is shifted to higher frequencies with the increasing of the Zn concentration, size of the nanoparticles and with ferrofluids containing ellipsoidal instead of spherical nanoparticles. However, the difference in the shifting of the PBS due to oblate or prolate ellipsoidal nanoparticles, is negligible. The effects of the Zn concentration, the width of the ferrofluid and air layers, as well as their dielectric constant on the PBS, allow us to propose photonic quantum wells (QWs) by means of which we can have very well defined frequency regions to transmit or reflect electromagnetic waves to be used in technological applications. We also extend our analysis considering dissipative effects in the ferrofluid layers, and we found a considerable reduction of the transmission power as the number N of layer period is increased.

1. INTRODUCTION

After works by Yablonovitch [1] and John [2] in which the photonic crystals were proposed, many experimental and theoretical works have been devoted to the understanding of the physical properties of these crystals. PCs are periodic structures characterized by the periodic variation of refractive index and the consequently periodic spacial variation of the dielectric constant, thus allowing the appearance of define frequency ranges and address for which the propagation of the electromagnetic waves is prohibited or permitted [3]. As a consequence, the tunability of PCs opens a new perspective in the scientific research and in technological applications. To obtain a tunable PC, the dielectric constant or the magnetic permeability of one of the constituents materials must depend on some external parameters, such as electric or applied magnetic fields [4, 5], temperature and hydrostatic pressure [6], applying mechanical force, stress, etc., which can modify the structure of this systems and consequently the optical response function of the PC.

In this work using the transfer matrix technique we study the photonic band structure of the 1D PCs made of alternating layers of air (layer 1) and ferrofluid (layer 2), which consists of cobalt-zinc ferrite nanoparticles $(\text{Co}_{1-x}\text{Zn}_x\text{Fe}_2\text{O}_4)$ coated by oleic acid suspended in the host liquid (ethanol), as a function of the Zn concentration, size and shape of the nanoparticles in the ferrofluid, which can be ellipsoids or spheres; we also study the optical response of photonic quantum wells [7] constructed using this type of ferrofluids.

2. THEORETICAL FRAMEWORK

In Figure 1(a) we display a scheme of a 1D photonic superlattice studied in this work.

The effective dielectric constant ε_{eff} of the whole suspension was obtain by the Maxwell-Garnett approximation (MGA) wich describes a three-component composite where many particles are randomly embedded in a host medium. To characterize the electromagnetic properties of the composite media, it is important to know the electromagnetic parameters of both the host material and the inclusions (nanoparticles). For a mixture of a base material with permittivity ε_e (ethanol), spherical nanoparticles with permittivity ε_f (cobalt-zinc ferrite), and coated with oleic acid of permittivity ε_a , the effective permittivity is [8]

$$\frac{\varepsilon_2 - \varepsilon_e}{\varepsilon_2 - 2\varepsilon_e} = (f_1 + f_2) \frac{f_1 (\varepsilon_a - \varepsilon_e) + f_2 t_{12} (\varepsilon_f - \varepsilon_e)}{f_1 (\varepsilon_a + 2\varepsilon_e) + f_2 t_{12} (\varepsilon_f - 2\varepsilon_e)}, \quad (1)$$

where $t_{12} = \frac{3\varepsilon_a}{\varepsilon_f + 2\varepsilon_a}$, f_1 and f_2 are the volume fractions of the coating and the core materials, respectively.

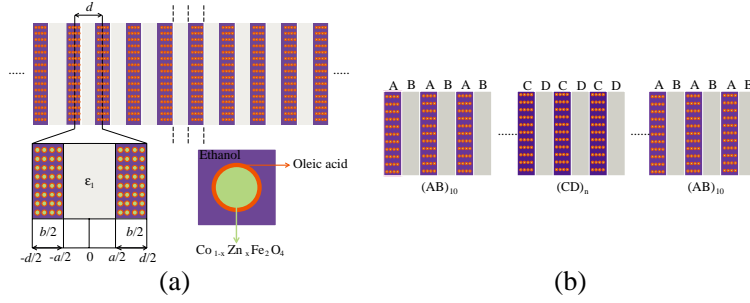


Figure 1: (Color online). (a) Pictorial view of the 1D photonic crystal, composed of alternating layers of air (layer 1) and ferrofluid (layer 2). In the ferrofluid layers, ferromagnetic spherical nanoparticles are embedded in a carrier fluid. For the model calculations, we take layer 1 to be air, the carrier fluid, ethanol, and the suspended nanoparticles, cobalt-zinc ferrites (core) coated by oleic acid (shell). (b) Esquematic view of a 1D photonic quantum well, $(AB)_{10}/(CD)_n/(AB)_{10}$, made of two different 1D photonic crystals with different Zn concentrations. The subindex 10 and n correspond to the number of repeated periods in the barriers and wells respectively.

For the three-phase mixtures we follow the MGA for two confocal inclusion phases (ε_f and ε_a) contained in a background representing the third phase (ε_e). The effective permittivity of an isotropic three-phases confocal system of ellipsoids was derived by Sihvola and Lindell [9] for any number of confocal ellipsoids, in the isotropic case as

$$\varepsilon_{eff} = \varepsilon_e + \frac{\frac{\varepsilon_e}{3} \sum_{i=a,b,c} \left(\frac{n_\nu \alpha^i}{\varepsilon_e} \right)}{1 - \frac{1}{3} \sum_{i=a,b,c} N_1^i \left(\frac{n_\nu \alpha^i}{\varepsilon_e} \right)}, \quad (2)$$

where

$$\frac{n_\nu \alpha^i}{\varepsilon_e} = (f_1 + f_2) \left[(\varepsilon_a - \varepsilon_e) + [\varepsilon_a + N_1^i (\varepsilon_e - \varepsilon_a)] \frac{(\varepsilon_f - \varepsilon_a) \frac{f_2}{f_1 + f_2}}{[\varepsilon_a + N_2^i (\varepsilon_f - \varepsilon_a)]} \right] \cdot \left[[\varepsilon_e + N_1^i (\varepsilon_a - \varepsilon_e)] + N_1^i (1 - N_1^i) (\varepsilon_a - \varepsilon_e) \cdot \frac{(\varepsilon_f - \varepsilon_a) \frac{f_2}{f_1 + f_2}}{[\varepsilon_a + N_2^i (\varepsilon_f - \varepsilon_a)]} \right]^{-1}, \quad (3)$$

a , b , and c are the three orthogonal axial directions of the ellipsoid, and N_i are the corresponding depolarization factors of the ellipsoid. For simplicity, we consider ellipsoids generated by the rotation of an ellipse around its major or minor axes, which produces prolate or oblate spheroids, correspondingly. These relations are plotted in the inset in Figure 2 as a function of the aspect ratio $m = \frac{a}{b}$. Similarly, the formulas used to calculate the effective permittivity ε are employed to calculate the effective permeability, owing to the separability of the electrostatic and magnetostatic problems which can be derived from Maxwell's equations [10].

3. RESULTS

In our calculations we have taken the ethanol dielectric constant and its refractive index to be 25.3 and 1.36, and the oleic acid dielectric constant and its refractive index equal to 2.34, and 1.44 respectively. For the dielectric constant of the cobalt-zinc ferrites nanoparticles as a function of the Zn concentration we have used the data given in reference [11], and for the magnetic permeability the data in reference [12].

Firstly, Figure 2(a) is devoted to show the PBS dependence with the radius of the nanoparticles, calculated by using Eq. (1). Note that for larger values of the radius, the PBS is shifted to higher frequencies except for the lower energy band, which means that the ferrofluid acquires higher values of the dielectric constant.

The shape effects of the nanoparticles on the PBS is presented in Figure 2(b), where we compare the results obtained for ferrofluids containing spherical, and ellipsoidal nanoparticles. According with Eq. (2), the dielectric constant of ferrofluids based on ellipsoids depends on the depolarization factor, which in turn depends on the aspect ratio $m = \frac{a}{b}$. It is noticeable that the PBS is shifted to higher energies in PC with ferrofluids containing ellipsoidal than spherical nanoparticles. On the

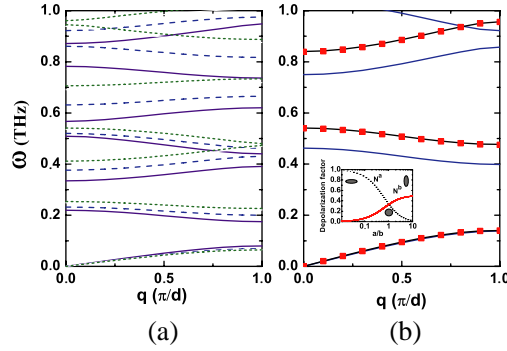


Figure 2: (Color online). (a) PBS of the PC varying the nanoparticles radius. The purple line (solid) is for $a_2 = 1.5$ nm with $f_2 = 0.2$, the blue line (dash) is for $a_2 = 3$ nm with $f_2 = 0.3$, and the green line (dot) is for $a_2 = 7.5$ nm with $f_2 = 0.4$. (b) PBS of the PC varying the nanoparticles shape. The blue line (solid) is for ferrofluids with spherical nanoparticles, the black line (solid) and red squares which superimpose themselves, are for ferrofluids with oblate and prolate ellipsoidal nanoparticles, respectively. The inset shows the depolarization factors N^a and N^b , of spheroidal nanoparticles as a function of the axial ratio of the spheroids, $m = \frac{a}{b}$.

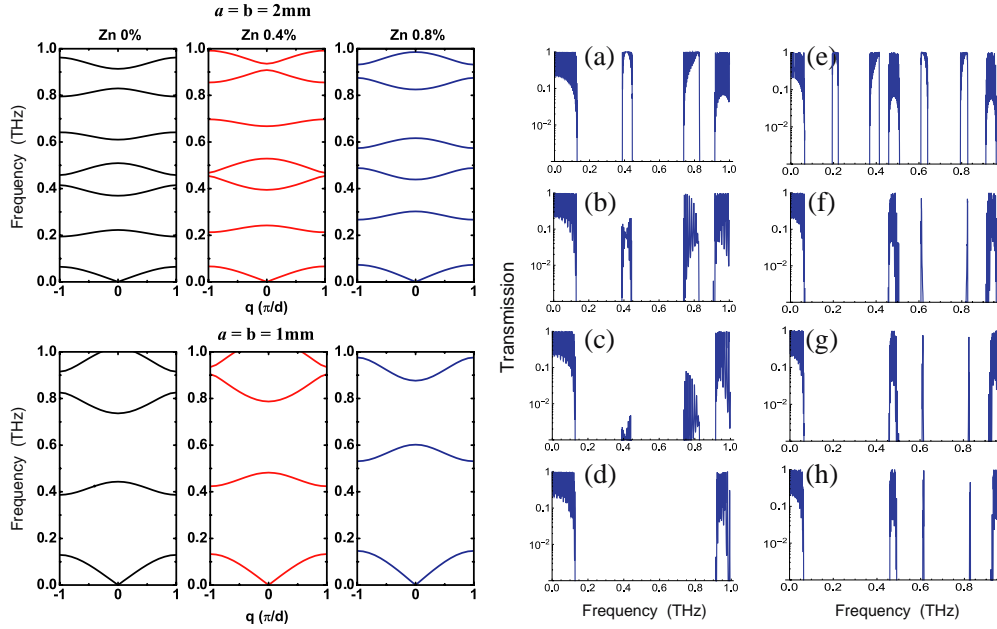


Figure 3: (Color online). Photonic band structure with alternating layers of air and ferrofluid, with different Zn concentration. The above panels are for $a = b = 2$ mm and down panels are for $a = b = 1$ mm. In panels (a)–(d), transmission in a photonic QW structures, $(AB)_{10}/(CD)_n/(AB)_{10}$, as a function of frequency with (a) $n = 0$, (b) $n = 1$, (c) $n = 2$, and (d) $n = 5$. $(CD)_n$ is the superlayer made of alternating layers of air and ferrofluid with $x = 0.8$ and $(AB)_m$ with $x = 0$, with $a = b = 1$ mm, and In panels (e)–(h), transmission in a photonic QW structures, $(AB)_{10}/(CD)_n/(AB)_{10}$, as a function of frequency with (a) $n = 0$, (b) $n = 5$, (c) $n = 7$, and (d) $n = 10$. In this case $(CD)_n$ and $(AB)_m$ are constructed with $a = b = 2$ mm.

other hand, no changes are observed between the PBS of PC with ferrofluids containing prolate or oblate ellipsoidal nanoparticles, due to the fact that the ferrofluid layer has the same filling factor in each case of the nanoparticles ordering.

In Figure 3, we investigate the effects of the Zn concentration (x) on the PBS of 1D photonic crystals taking into account the variation of the dielectric constant with the Zn concentration in the nanoparticles, as it is displayed in Table 1. The dielectric constant of the ferrofluid layer decreases with the increment of the Zn concentration, shifting the PBS to higher frequencies, in agreement with the electromagnetic variational theorem [3]. Otherwise, it is observed that for a given Zn concentration the PBS is shifted to higher frequencies with the diminishing of the layer widths.

As observed in Figure 3, the second and third band of the PBS with $x = 0$ for $a = b = 1$ mm are

just inside the first and second photonic band gap (PBGs) of the PBS with $x = 0.8$, respectively, while the second band of the PC with $x = 0.8$ is just inside the second band gap (BG) of the PBS with $x = 0$. Also, it is noticed that the second, third, fourth and sixth band of the PBS with $x = 0$ and ($a = b = 2$ mm) fall within the first and second BG of the PBS with $x = 0.8$ for $a = b = 1$ mm. We use these findings to propose photonic QW structures, which may present large forbidden PBGs with weak transmission, or at the contrary, frequency regions where the transmission is sharp but very high. This opens the prospect of applications of these PC in the design of new optical devices.

In what follows, we name $(AB)_m$ the superlayer made of m alternating layers of air and ferrofluid with $x = 0$, and $(CD)_n$ the superlayer made of n alternating layers of air and ferrofluid with $x = 0.8$, both with $a = b = 1$ mm. The constructed structure is $(AB)_m/(CD)_n/(AB)_m$, where the CD layer can play the role of barrier or well. As mentioned above, in these structures some well bands for photonic propagation are inside the photonic gap of the barriers.

The transmission spectra of a photonic QW structure as a function of frequency is presented in Figures 3(a)–(h). As the band gaps of the $(CD)_n$ superlattice cannot sustain the propagation of electromagnetic waves with frequencies inside its PBGs, the transmission falls to zero with the increasing of the penetration depth, that is, increasing the number of layers in this region. In this case, the photon is not allowed to propagate through the barrier slab of the PC. In the absence of CD layers [Figure 3(a)] there is a large transmission through all bands of the $(AB)_m$ superlattice, whereas the transmission is reduced to zero for frequencies between 0.15 THz to 0.93 THz with the increase of the $(CD)_n$ superlattice width, as depicted in Figures 3(b)–3(d). Also, in Figure 3 it is important to note that in absence of the CD superlattice, the $(AB)_m$ one presents a complete transmission between 0.91 THz and 1.1 THz in its last band (Figure 3(a)), by increasing the number of CD layers, this transmission finding with the last transmission band of CD layers that go from 0.84 THz to 0.99 THz as shown in the PBS, the final result when increasing the CD layers is a transmission band between 0.91 THz and 0.99 THz of Figure 3(d) where the bands overlap in frequency rang.

In addition, when the thickness of the layers is varied, namely, taking $(AB)_m$ and $(CD)_n$ as the superlattices made of alternating layer of air and ferrofluid with $x = 0$ and $x = 0.8$ respectively, both with $a = b = 2$ mm, it is found the same behavior, that is, zero transmission coefficient for frequencies in the gap region. In Figures 3(g) and 3(h), two maximum-transmission sharp peaks close to 0.61 THz and 0.83 THz are observed, which can be used as high-quality filters.

Finally, In Figure 4, we present results considering dissipative effects in the ferrofluid layers by adding a complex term in the dielectric constant, finding a considerable reduction of the transmission power as the number N of layer period is increased. We obtain these results by taking the

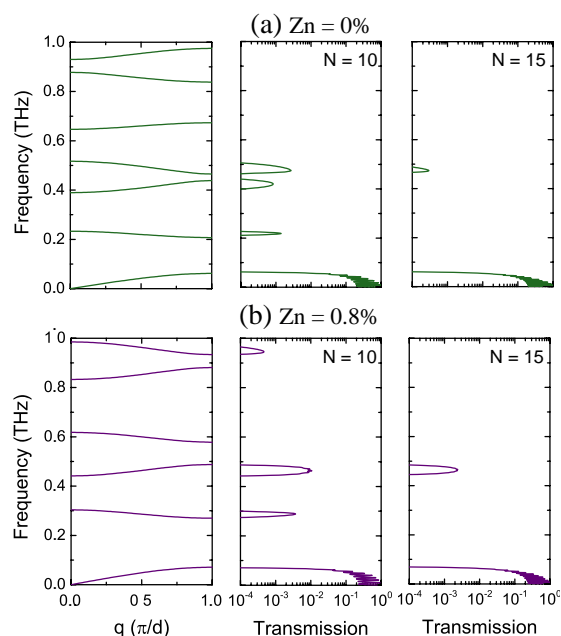


Figure 4: (Color online). PBS and transmittance in 1D PC with $a = b = 2$ mm, calculated including the complex term in the ferrite dielectric constant. Panels (a) are for $x = 0$, and (b) are for $x = 0.8$, respectively.

complex dielectric constants of CoFe_2O_4 and $\text{Co}_{0.2}\text{Zn}_{0.8}\text{Fe}_2\text{O}_4$ from reference [11], where the former is higher than the latter, result which is in agreement with the high dissipative energy effects in the CoFe_2O_4 .

4. CONCLUSION

In summary, based on the transfer matrix method, we theoretically studied the PBS in 1D PCs, composed of alternating layers of air and a ferrofluid containing ($\text{Co}_{1-x}\text{Zn}_x\text{Fe}_2\text{O}_4$) nanoparticles coated by oleic acid suspended in ethanol. We have found that the PBGs are shifted to higher frequencies with the increase of the Zn concentration and the size of the nanoparticles. In addition, we found that in PCs containing ferrofluids the PBS is shifted to higher frequencies in those containing ellipsoidal instead of spherical nanoparticles, however the difference in the shifting of the PBS due to oblate or prolate ellipsoidal nanoparticles, is negligible. Also, taking into account the effects of the Zn concentration on the PBS, we proposed photonic QWs, which depending on their composition can offer large forbidden gaps, but with sharp transmission peaks, with very well defined frequency ranges which can be used in several technological application. We also extend our analysis considering dissipative effects in the ferrofluid layers, finding a considerable reduction of the transmission power as the number N of layer period is increased. We hope experimental work on these subjects confirm our findings, which certainly can be taken into account to be used in future technological applications.

ACKNOWLEDGMENT

One of us L. E. G. thanks to Colciencias, the Colombian Cientific Agency for economic suport.

REFERENCES

1. Yablonovitch, E., "Inhibited spontaneous emission in solid-state physics and electronics," *Phys. Rev. Lett.*, Vol. 58, 2059–2062, 1987.
2. John, S., "Strong localization of photons in certain disordered dielectric superlattices," *Phys. Rev. Lett.*, Vol. 58, 2486–2489, 1987.
3. Joannopoulos, J. D., et al., *Photonic Crystals: Molding the Flow of Light*, Princeton University Press, Princeton, 1995.
4. Lopez, J., L. E. González, M. F. Quiñonez, M. E. Gómez, N. Porrás-Montenegro, and G. Zambrano, "Magnetic field role on the structure and optical response of photonic crystals based on ferrofluids containing $\text{Co}_{1-x}\text{Zn}_x\text{Fe}_2\text{O}_4$ nanoparticles," *J. Appl. Phys.*, Vol. 115, 193502, 2014.
5. Lopez, J., L. E. González, M. F. Quiñonez, M. E. Gómez, N. Porrás-Montenegro, and G. Zambrano, "Band structure of a 2D photonic crystals based on ferrofluids of $\text{Co}_{0.8}\text{Zn}_{0.2}\text{Fe}_2\text{O}_4$ nanoparticles under perpendicular applied magnetic fields," *J. Phys.: Conf. Ser.*, Vol. 480, 012033, 2014.
6. González, L. E. and N. Porrás-Montenegro, "Pressure, temperature and plasma frequency effects on the band structure of a 1D semiconductor photonic crystal," *Physica E*, Vol. 44, 773–777, 2012.
7. Zi, J., J. Wan, and C. Zhang, "Large frequency range of negligible transmission in 1D photonic quantum well structures," *Appl. Phys. Lett.*, Vol. 73, 2084–2086, 1998.
8. Sihvola, A. H. and I. V. Lindell, "Polarizability modeling of heterogeneous media," *Progress In Electromagnetics Research*, Vol. 6, 101–151, 1992.
9. Sihvola, A. and I. V. Lindell, "Polarizability and effective permittivity of layered and continuously inhomogeneous dielectric ellipsoids," *Journal of Electromagnetic Waves and Applications*, Vol. 4, No. 1, 1–26, 1990.
10. Sihvola, A. H. and I. V. Lindell "Effective permeability of mixtures," *Progress In Electromagnetics Research*, Vol. 6, 153–180, 1992.
11. Ramana Murty, S., "Dielectric behaviour of cobalt-zinc ferrites," *J. Mater. Sci. Lett.*, Vol. 3, 1049–1051, 1984.
12. Dong, H., A. Meininger, H. Jiang, K.-S. Moon, and C. P. Wong, "Magnetic nanocomposite for potential ultrahigh frequency microelectronic application," *J. Electron. Mater.*, Vol. 36, 593–597, 2007.